Intramolecular Stacking of Two Aromatic Rings in the Platinum(II) Coordination Sphere: Preparation, Crystal Structures, and ^{1}H NMR Spectra of Bipyridine(*N*-arylmethyl-1,2-ethanediamine)platinum(II) Nitrate

Masafumi Goto,* Takashi Matsumoto, Masamitsu Sumimoto, and Hiromasa Kurosaki

Faculty of Pharmaceutical Sciences, Kumamoto University, Oe-honmachi, Kumamoto 862-0973

(Received May 24, 1999)

Square-planar complexes with the formula $[Pt(L_1)(L_2)](NO_3)_2 \cdot nH_2O$, where L_1 is bipyridine (bpy) and L_2 is *N*-benzyl-1,2-ethanediamine (Been) (**1**) (n = 0), *N*-(1-naphthyl)methyl-1,2-ethanediamine (Npen) (**2**) (n = 2), and *N*-(9-anthryl)methyl-1,2-ethanediamine (Aten) (**3**) (n = 2), were prepared and X-ray crystal-structure determinations were carried out. The molecular structures of the complex cations revealed that the *N*-arylmethyl groups are forced to take pseudo axial dispositions due to an intramolecular repulsion from hydrogen atoms of bpy. The aromatic–aromatic interaction between the aromatic rings of ethanediamine derivatives and coordinated bpy caused **2** and **3** to take a conformation where the aromatic ring and bpy stack face-to-face to each other intramolecularly. An intermolecular aromatic–aromatic face-to-face interaction was also observed for **1**, **2**, and **3** in the crystals. The latter interaction occurs between bpy and the aryl substituent, except for **1**. For D_2O solutions of **1** through **3**, significant upfield shifts due to the intramolecular stacking were observed in the ^{1}H NMR spectra for the protons on the half ring of bipyridine, depending on the size of the aromatic ring. The crystal data of **1**: monoclinic, $P2_1/c$, a = 9.884(2), b = 24.717(2), c = 9.560(5) Å, β = 113.83(3)°, Z = 4, and R = 0.029. **2**: monoclinic, Ia, a = 17.030(5), b = 10.461(4), c = 14.727(4) Å, β = 94.72°, Z = 4, and R = 0.023. **3**: monoclinic, Pn, a = 10.471(2), b = 8.844(5), c = 15.332(3) Å, β = 98.61(2)°, Z = 2, and R = 0.034.

Biopolymers, such as proteins and nucleic acids, build specific three-dimensional structures to function. Though the primary structure defines a molecule, the integration of the weak interaction makes these three-dimesional structures. These weak interactions are classified as Coulombic (electrostatic), hydrogen bond, van der Waals, and hydrophobic interactions. One approach to evaluate these interactions is to construct low-molecular model compounds which allow a detail inspection. The coordination compounds have an advantage in this purpose, because several building blocks, ligands, can be assembled by metal center(s) which have specific geometrical preference. The central metal ions play a role of templates.

Sigel and his co-workers have shown that the aromatic–aromatic interaction plays an important role in the formation of ternary metal complexes.[1—3] Odani and Yamauchi have demonstrated the importance of this interaction in constructing ternary metal complexes with an aromatic diimine, such as bipyridine (bpy) and 1,10-phenanthroline (phen), and a biomolecule, such as amino acids, peptides, and nucleotides.[4—9]

Platinum(II) has unique properties: a strong tendency to form square-planar four-coordinated compounds, inertness in substitution, and diamagnetism. These enable us to examine structures of these complexes in detail through the NMR method as well as crystallography. The platinum compounds are also important in terms of the development of anticancer agents, such as cisplatin. The positively charged platinum complexes with aromatic ligands, such as bpy, have been shown to intercalate double-stranded DNA by Lippard.[10] Odani and Yamauchi have investigated the interaction of platinum complexes bearing an aromatic-ring moiety and several nucleoside 5′-monophosphate (NMP),[11,12] and have shown that $[Pt(bpy)(en)]^{2+}$ and $[Pt(phen)(en)]^{2+}$ stacks with adenosine 5′-monophosphate (AMP), guanosine 5′-monophosphate (GMP), and cytidine 5′-monophosphate (CMP) in dilute aqueous solution and that the equilibrium constant is larger than those between bpy and NMP or the self stacking of AMP. This is ascribed to charge-transfer from the purine ring to electron-deficient coordinated bpy and phen.[11,12]

We chose *N*-arylmethyl-1,2-ethanediamine and bpy as ligands and platinum(II) as the metal ion to construct a series of ternary complexes with the formula $[Pt(bpy)(L)]^{2+}$, where L stands for *N*-arylmethyl-1,2-ethanediamine, in order to clarify the nature of the aromatic–aromatic ring interaction, particularly the intramolecular one, because of the ease of a systematic variation of the ligands. In this report, the results of X-ray crystallography and an ^{1}H NMR study of deuterium oxide solutions of ternary complexes with three *N*-arylmethyl-1,2-ethanediamines (shown in Fig. 1) are described.

Experimental

Materials. (Bipyridine)dichloroplatinum(II) was prepared according to the method of Morgan and Burstall.[13] (Bipyridine)(1,

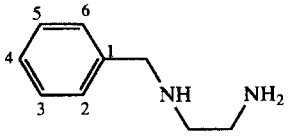

N-benzyl-1,2-ethanediamine(Been)

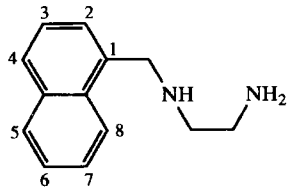

N-(1-naphthyl)methy-1,2-ethanediamine(Npen)

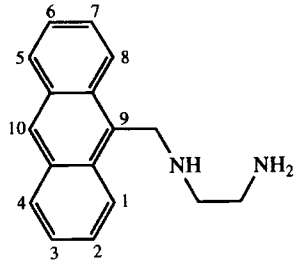

N-(9-anthryl)methyl-1,2-ethanediamine(Aten)

Fig. 1. The structural formula of *N*-Arylmethyl-ethanediamines.

2-ethanediamine)platinum(II) nitrate was prepared according to a method from the literature.[13,14] *N*-Benzyl-1,2-ethanediamine, 1,2-ethanediamine, 1-chloromethylnaphthalene, and 9-hydroxymethylanthracene were purchased from Tokyo Kasei and used without further purification. ^{1}H and ^{13}C NMR spectra were recorded with a JEOL GX-400 spectrometer using sodium trimethylsilylpropionate-2,2,3,3-d_4 (TSP) and dioxane as internal standards, respectively.

Preparation of Ethanediamine Derivatives. *N*-(1-Naphtyl)-methyl-1,2-ethanediamine Monohydrochloride. To well-stirred dehydrated ethanediamine (50.4 g, 0.839 mol), 1-chloromethylnaphthalene (14.8 g, 0.0839 mol) was added dropwise at room temperature. After complete addition, the temperature of the reaction mixture was raised to 117 °C and the mixture was refluxed for 1 h. The mixture was cooled and the excess of ethanediamine was evaporated under reduced pressure. The mixture turned to an heterogeneous residue upon evaporation, and then turned to a clear solution again. Ethanol (50 cm^3) was added to the solution and the mixture was allowed to stand overnight. Separated crystals were collected on a filter by suction, washed with cold ethanol, and dried in a desiccator. Yield, 8.62 g (43.4%). Found: C, 65.20; H, 7.34; N, 12.28%. Calcd for $C_{13}H_{16}N_2$: C, 65.96; H, 7.24; N, 11.83%. UV λ_{max}/nm (ε/cm^{-1} M^{-1}) (1 M = 1 mol dm^{-3}) 312 (3.79×10^2), 280 (5.88×10^3), 271 (5.05×10^3), 221 (6.59×10^4). ^{1}H NMR (dmso-d_6) δ = 2.86 (multiplet), 2.90 (multiplet), 4.17 (s), 7.48 (t), 7.52 (t), 7.54 (t), 7.58 (d), 7.82 (d), 7.93 (d), 8.17 (d). ^{13}C NMR (D_2O) δ = 39.20, 46.48, 50.16, 124.05, 126.57, 127.08, 127.60, 127.87, 129.27, 129.66, 131.85, 134.16, 134.40.

9-Chloromethylanthracene. To a dehydrated methylene chloride solution of 9-hydroxymethylanthracene (5.00 g, 24.0 mmol) in 100 cm^3, 1.1 equivalent of thionyl chloride (3.1 g, 26.4 mmol) was added dropwise at room temperature. The reaction mixture was refluxed for 2 h, and then concentrated; the remaining residue was dissolved in a ca. 30 cm^3 portion of methylene chloride. The methylene chloride solution was extracted with an aq 5% sodium hydrogencarbonate solution (ca. 20 cm^3). The methylene chloride was evaporated from the reaction mixture and the remaining white precipitate was collected on a filter. Yield, 4.78 g (87.9%).

***N*-(9-Anthranyl)methyl-1,2-ethanediamine Dihydrochloride.** A benzene solution of 9-chloromethylanthracene (4.00 g, 17.7 mmol, 10 cm^3) was added to ethanediamine (10.8 g, 0.179 mol) dropwise at room temperature and the mixture was refluxed for 2 h. The proceeding of the reaction was followed by TLC (developing agent: methylene chloride : methanol = 2 : 0.25). Excess ethanediamine was evaporated under reduced pressure. The remaining oily residue was washed with an aqueous solution saturated with sodium hydrogencarbonate (20 cm^3) and aqueous solution saturated with sodium chloride and dehydrated with magnesium sulfate. After removing the solvent, 1 M hydrochloric acid (40 cm^3) was added. The separated precipitates were collected on a filter. These precipitates were recrystallized from a mixture of water (10 cm^3) and ethanol (50 cm^3). Yield, 2.98 g (58.8%). UV λ_{max}/nm (ε/cm^{-1} M^{-1}) 387 (6.20×10^3), 367 (7.21×10^3), 350 (5.27×10^3), 335 (2.92×10^3), 254 (1.72×10^5).

Preparation of Platinum(II) Complexes. [Pt(bpy)(Been)]-$(NO_3)_2$ (1). To a suspension of [$PtCl_2$(bpy)] (301.6 mg, 0.71 mmol) in 13 cm^3 of water, Been (108.6 mg, 0.71 mmol) was added. After being stirred at 80 °C for 2 h, the mixture turned into a yellow solution. This was allowed to cool and was then filtered to remove small amounts of undissolved materials. An equivolume of an aqueous solution saturated with sodium nitrate was added. After allowing to stand overnight at room temperature, yellow crystals were separated, filtered, washed with 0.05 M nitric acid, and dried. Yield, 421 mg (93.2%). Found: C, 36.25; H, 3.52; N, 13.37%. Calcd for [$Pt(C_{10}H_8N_2)(C_9H_{14}N_2)$]$(NO_3)_2$: C, 36.48; H, 3.55; N, 13.44%. UV λ_{max}/nm (ε/cm^{-1} M^{-1}) 319.0 (1.65×10^4), 308.1 (1.21×10^4), 243.9 (2.07×10^4).

[Pt(bpy)(Npen)]$(NO_3)_2\cdot2H_2O$ (2). To a suspension of [$PtCl_2$(bpy)] (422 mg, 1.00 mmol) in water (6 cm^3), Npen·HCl (308 mg, 1.3 mmol) and sodium carbonate (126 mg, 1.5 mmol) was added and the mixture was stirred at 80 °C. After 15 min, the dichloroplatinum complexes reacted with the diamine and the mixture turned to a yellow solution. After cooling to room temperature, an equivolume of saturated sodium nitrate was added and allowed to stand overnight. A yellow oil was separated. The supernatant was discarded by decantation and water (5 cm^3) was added to dissolve the oil and ethanol (5 cm^3) was added further. The mixture was allowed to stand in a refrigerator overnight. Separated yellow crystals were collected on a filter, washed with small amounts of cold ethanol and ether successively. Yield, 415 mg (58.4%). Found: C, 38.80; H, 3.83; N, 11.85%. Calcd for [$Pt(C_{10}H_8N_2)$-$(C_{13}H_{16}N_2)$]$(NO_3)_2\cdot2H_2O$: C, 38.82; H, 3.97; N, 11.81%. UV λ_{max}/nm (ε/cm^{-1} M^{-1}) 319.2 (1.19×10^4), 307.7 (1.02×10^4), 296.4 (9.19×10^3), 221.8 (5.67×10^4), 206.4 (5.61×10^4).

[Pt(bpy)(Aten)]$(NO_3)_2\cdot2H_2O$ (3). To a suspension of [$PtCl_2$(bpy)] (422 mg, 1.00 mmol) in 8 cm^3 of water, Aten·2HCl (421 mg, 1.30 mmol) and sodium hydrogencarbonate (127 mg, 1.20 mmol) were added. The mixture was heated at 80 °C for 2 h until it turned to a pale-yellow solution. After the solution had cooled to room temperature, separated yellow precipitates were

collected on a filter. These were recrystallized from a mixture of water (6 cm^3) and ethanol (38 cm^3), separated yellow needles were collected on a filter, washed with ethanol, and dried under vacuum. Yield, 491 mg (68%). Found: C, 45.30; H, 4.02; N, 7.81%. Calcd for $[Pt(C_{10}H_8N_2)(C_{17}H_{18}N_2)]Cl_2 \cdot 2.5H_2O$: C, 45.19; H, 4.35; N, 7.81%. UV λ_{max}/nm (ε/cm^{-1} M^{-1}) 391.6 (4.48×10^3), 373.1 (5.26×10^3), 354.9 (5.03×10^3), 320.7 (1.49×10^4), 310 (1.18×10^4), 256.0 (1.11×10^5).

These were converted to nitrate salts by the addition of a saturated sodium nitrate solution to an equivolume aqueous solution of chloride salt (200 mg in 20 cm^3). Separated yellow precipitates were collected and recrystallized from a 1 : 1 water–ethanol mixture. Yellow crystals were collected on a filter, washed with ethanol, and dried under vacuum. Found: C, 42.47; H, 4.05; N, 10.76%. Calcd for $[Pt(C_{19}H_8N_2)(C_{17}H_{18}N_2)](NO_3)_2 \cdot 2H_2O$: C, 42.58; H, 3.97; N, 11.03%.

X-Ray Crystallographic Study of 1, 2, and 3. Crystals suitable for diffraction studies were grown by slow cooling of aqueous solutions (for **2** and **3**) or by slow cooling of an ethanol–aqueous solution (**1**), and were mounted on a thin glass fiber with epoxy resin. Data were collected on a Rigaku AFC-7R diffractometer at 20±1 °C. The final cell dimensions were obtained by a least-squares fit to the automatically centered settings for 20 reflections. Three reflections were monitored during data collection for each crystal. The intensity data were all corrected for absorption (empirically, based on azimuthal scans of several reflections), anomalous dispersion, and Lorentz and polarization effects. The space-group choice for each complex was unambiguously determined, but the space-group for **2** was converted from *Cc* to *Ia* during the course of refinement. The crystallographic data are summarized in Table 1.

The structure of **1** was solved by a heavy metal method on a Patterson map; those of **2** and **3** were solved by a direct method (SAPI).[15] A subsequent least-squares refinement and difference Fourier calculations revealed the atomic positions of the remaining non-hydrogen atoms. In the final cycle of the least-squares, the non-hydrogen atoms were refined with anisotropic thermal coefficients. For **1**, one of the two crystallographically independent nitrate ions was found to be disordered: one of the oxygen atoms and the nitrogen atom form an axis common to the two disordered structures, which are triangles rotated by 120° to each other. The hydrogens were fixed at the calculated positions. Tables of the final anisotropic thermal factors for all non-hydrogen atoms and the positions of the hydrogen atoms, bond lengths and angles, torsion angles, and the observed and calculated structure factor amplitudes are deposited as Document No. 73002 at the Office of the Editor of Bull. Chem. Soc. Jpn. Crystallographic data have been deposited at the CCDC, 12 Union Road, Cambridge CB2 1EZ, UK and copies can be obtained on request, free of charge, by quoting the publication citation and the deposition numbers 135920-135922.

Results and Discussion

Reactions of $[PtCl_2(bpy)]$ with three ethanediamine derivatives (*N*-benzyl-1,2-ethanediamine, *N*-(1-naphthyl)-methyl-1,2-ethanediamine, and *N*-(9-anthranyl)methyl-1,2-ethanediamine) took place in the usual manner[13] and the ternary platinum(II) complexes (**1**, **2**, and **3**) were isolated as nitrate salts.

The crystallography of **1**, **2**, and **3** was carried out to obtain information about the structure of the platinum(II) complexes with bpy and *N*-arylmethyl-1,2-ethanediamine. The fractional coordinates of **1** to **3** are tabulated in Tables 2, 3, and 4. Perspective drawings and labeling of the nonhydrogen atoms are shown in Fig. 2. These complexes have typical square-planar structures around the platinum center with the coordination of two imino nitrogens of bpy and the two amines of the ethanediamine derivatives. Comparison of the bond lengths and bond angles around the platinum

Table 1. Summary of Crystallographic Data for $[Pt(bpy)L](NO_3)_2 \cdot nH_2O$

L (Complex)	Been (**1**)	Npen (**2**)	Aten (**3**)
Formula	$C_{19}H_{22}N_6O_6Pt$	$C_{23}H_{28}N_6O_8Pt$	$C_{27}H_{30}N_6O_8Pt$
Molecular weight	625.51	711.60	761.66
Cryst. syst.	Monoclinic	Monoclinic	Monoclinic
Space group	$P2_1/c$	*Ia*	*Pn*
a/Å	9.884(2)	17.030(5)	10.471(2)
b/Å	24.717(2)	10.461(4)	8.844(5)
c/Å	9.560(5)	14.727(4)	15.332(3)
β/°	113.83(3)	94.72(1)	98.61(2)
V/Å^3	2136(2)	2614(1)	1403.9(8)
Z	4	4	2
d(calc)	1.945	1.808	1.802
μ/mm^{-1}	6.59	5.403	5.038
Radiation, λ/Å	Mo $K\alpha$, 0.71069	Mo $K\alpha$, 0.71069	Mo $K\alpha$, 0.71069
crystal dimensions/mm^3	$0.20\times0.20\times0.20$	$0.18\times0.15\times0.09$	$0.21\times0.15\times0.15$
T/K	293(1)	293(1)	293(1)
$2\theta_{max}$/°	55.0	55.0	55.0
Transmission factor	0.86—1.00	0.80—1.00	0.79—1.00
No. of obsd reflcns	5324	3257	3617
No. of unique reflcns	5038	3173	3436
No. of obsd reflcns ($I > 3\sigma(I)$)	3365	2610	2708
R[a)]	0.029	0.023	0.034
R_w[b)]	0.021	0.027	0.060

a) $R = \sum||F_o| - |F_c||/\sum|F_o|$. b) $[\sum w(|F_o| - |F_c|)_2/\sum w|F_o|^2]^{1/2}$, $w = 1/\sigma^2(F_o)$.

Table 2. Fractional Coordinates and B(eq) of [Pt(bpy)(Been)]$(NO_3)_2$ (**1**)

Atom	x	y	z	B (eq)/Å^2
Pt(1)	0.20088(3)	0.112136(9)	0.09423(3)	4.690(6)
O(1)	0.1510(7)	0.1802(2)	0.4150(7)	11.7(2)
O(2)	0.1324(7)	0.2567(3)	0.485(1)	17.1(3)
O(3)	0.3123(6)	0.2398(2)	0.4408(6)	9.3(2)
O(4)	0.4486(5)	−0.0071(2)	0.7453(6)	9.4(2)
O(5)[a]	0.271(2)	0.023(1)	0.547(2)	10.3(4)
O(6)[a]	0.479(2)	0.0569(9)	0.616(2)	12.6(5)
O(7)[b]	0.288(4)	0.055(2)	0.617(4)	7.1(8)
O(8)[b]	0.451(5)	0.021(2)	0.551(5)	11(1)
N(1)	0.0637(5)	0.1121(2)	−0.1297(5)	5.2(1)
N(2)	0.0284(5)	0.0731(2)	0.1078(6)	4.8(1)
N(3)	0.3301(5)	0.1129(2)	0.3221(5)	6.3(1)
N(4)	0.3753(5)	0.1527(2)	0.0795(5)	5.0(1)
N(5)	0.2002(8)	0.2249(3)	0.4477(8)	7.6(2)
N(6)	0.3968(8)	0.0237(3)	0.6382(8)	6.3(2)
C(1)	−0.0665(7)	0.0853(2)	−0.1608(7)	5.0(2)
C(2)	−0.1702(7)	0.0799(3)	−0.3144(9)	6.8(2)
C(3)	−0.1354(8)	0.1019(4)	−0.4264(8)	8.9(3)
C(4)	−0.0078(9)	0.1301(4)	−0.3932(9)	9.2(3)
C(5)	0.0893(7)	0.1356(3)	−0.2446(9)	7.0(2)
C(6)	−0.0869(7)	0.0644(2)	−0.0305(7)	4.6(2)
C(7)	−0.2137(7)	0.0378(2)	−0.0423(8)	5.6(2)
C(8)	−0.2201(8)	0.0190(2)	0.091(1)	6.5(2)
C(9)	−0.1072(8)	0.0289(3)	0.2285(8)	6.4(2)
C(10)	0.0176(7)	0.0557(2)	0.2343(7)	5.5(2)
C(11)	0.4786(7)	0.1359(3)	0.3507(8)	7.5(2)
C(12)	0.4590(7)	0.1771(3)	0.231(1)	6.9(2)
C(13)	0.4682(6)	0.1196(2)	0.0207(7)	5.5(2)
C(14)	0.5802(7)	0.1521(2)	−0.0135(8)	5.1(2)
C(15)	0.5421(6)	0.1699(3)	−0.1630(8)	5.9(2)
C(16)	0.6434(9)	0.1987(3)	−0.2016(8)	6.8(2)
C(17)	0.781(1)	0.2098(3)	−0.091(1)	8.1(3)
C(18)	0.8209(8)	0.1928(3)	0.057(1)	7.2(2)
C(19)	0.7205(7)	0.1636(3)	0.0931(8)	6.0(2)

a) occupancy, 0.724; b) occupancy, 0.276.

Table 3. Fractional Coordinates and B(eq) of [Pt(bpy)(Npen)]$(NO_3)_2 \cdot 2H_2O$ (**2**)

Atom	x	y	z	B (eq)/Å^2
Pt(1)	0.0061	0.06059(2)	0.0040	3.279(5)
O(1)	−0.2557(5)	0.160(1)	0.2120(6)	8.0(2)
O(2)	−0.3785(5)	0.124(1)	0.2261(6)	7.7(2)
O(3)	−0.3439(5)	0.1973(8)	0.0999(5)	6.5(2)
O(4)	0.3626(5)	0.2994(9)	−0.0613(6)	7.5(2)
O(5)	0.4505(6)	0.2371(9)	−0.1439(6)	8.1(3)
O(6)	0.3470(5)	0.325(1)	−0.2045(6)	9.5(3)
O(7)	0.2788(7)	0.5606(9)	−0.1101(8)	8.1(3)
O(8)	−0.1975(4)	0.2310(8)	0.5308(5)	6.6(2)
N(1)	0.0238(4)	0.2412(6)	−0.0403(4)	3.6(1)
N(2)	0.0957(6)	0.030(1)	−0.0764(6)	3.8(2)
N(3)	−0.0079(4)	−0.1247(7)	0.0440(5)	4.1(2)
N(4)	−0.0759(5)	0.0950(8)	0.0961(6)	3.2(2)
N(5)	−0.3259(5)	0.1585(7)	0.1805(6)	5.1(2)
N(6)	0.3874(6)	0.2843(8)	−0.1385(6)	5.3(2)
C(1)	0.0903(5)	0.2557(9)	−0.0815(5)	3.8(2)
C(2)	0.1141(6)	0.376(1)	−0.1091(6)	4.9(2)
C(3)	0.0670(7)	0.481(1)	−0.0956(7)	5.2(2)
C(4)	−0.0015(7)	0.4614(9)	−0.0562(7)	5.2(2)
C(5)	−0.0223(5)	0.3412(8)	−0.0280(6)	4.4(2)
C(6)	0.1338(6)	0.137(1)	−0.0977(6)	4.0(2)
C(7)	0.2049(5)	0.130(1)	−0.1342(7)	5.3(2)
C(8)	0.2375(6)	0.013(1)	−0.1513(7)	6.4(3)
C(9)	0.1947(7)	−0.098(1)	−0.1340(7)	6.0(3)
C(10)	0.126(1)	−0.085(1)	−0.094(1)	5.0(3)
C(11)	−0.0662(7)	−0.135(1)	0.1148(7)	4.5(2)
C(12)	−0.1212(8)	−0.026(1)	0.1020(9)	4.0(2)
C(13)	−0.0410(5)	0.135(1)	0.1899(6)	4.4(2)
C(14)	−0.0099(5)	0.2706(8)	0.1914(5)	4.1(2)
C(15)	0.0679(5)	0.2974(8)	0.1712(5)	4.0(2)
C(16)	0.0903(6)	0.4295(9)	0.1633(6)	4.5(2)
C(17)	0.0360(7)	0.5250(9)	0.1824(7)	5.6(3)
C(18)	−0.0375(6)	0.496(1)	0.2037(8)	5.7(3)
C(19)	−0.0596(5)	0.366(1)	0.2073(7)	5.0(2)
C(20)	0.1264(5)	0.205(1)	0.1577(6)	4.9(2)
C(21)	0.1986(6)	0.239(1)	0.1336(7)	6.3(3)
C(22)	0.2184(7)	0.367(2)	0.123(1)	6.5(3)
C(23)	0.1674(7)	0.460(1)	0.1359(7)	5.4(3)

centers are given in Table 5. The bond lengths of Pt–N are in the range of the expected values for **1** and **2**, but the bond lengths between Pt and the nitrogen atoms (N(3) and N(4)) of the ethanediamines increased with the reduction in length of Pt–N(1) and Pt–N(2) for **3**.[16,17] Accompanying this, the bond angles of N(3)–Pt–N(4) becomes narrower (83.5(2), 82.8(3), and 79.4(4)° and the bond angle of N(2)–Pt–N(3) becomes wider (96.8(2), 97.5(4), and 98.6(4)°) through **1** to **3**.

Intramolecular stacking between one of the pyridine rings of bpy and the naphthalene or anthracene ring is seen for **2** and **3** from the close separation between the bpy and the aromatic rings. The phenyl group of **1** situates in a region far from the metal center.

The distortion of coordinated bpy is evaluated by the displacement of each non-hydrogen atom from the least-squares plane defined by Pt, N(1), N(2), N(3), and N(4). For **1**, all non-hydrogen atoms of bpy lie in this plane with a deviation of less than 0.1 Å. For **2** and **3**, N(1), C(6), and C(5) are located at the opposite side by 0.4 Å, but the carbon atoms in the other ring of bpy, C(7) and C(8), are located at the same side with deviations of up to 0.85 Å with respect to the naphthalene or anthracene ring. The dihedral angles between two pyridine rings of bpy are 2.4, 9.9, and 11.2°, respectively. These displacements are not caused by the torsion of N(1)–C(1)–C(6)–N(2), because these torsion angles are −1.2, 6, and −1°, for **1**, **2**, and **3**, respectively. The bpy takes a saddle-like deformation for **2** and **3**.

The ethanediamine derivatives within **1** to **3** take gauche conformations with torsion angle of −52, −49, and −53° for N(3)–C(11)–C(12)–N(4). While the carbon atom next to the primary amine, C(11), shows small deviations from the least-squares plane of Pt, N(1), N(2), N(3), and N(4), i.e., 0.07 Å for **2** to 0.09 Å for **1**, the carbon next to the secondary amine, C(12), shows larger deviations from this plane: −0.56, −0.51, and −0.44 Å for **1**, **2**, and **3**, respectively. The carbon atom of C(13) locates at 1.30, 1.48, and 1.53 Å above this plane for **1**, **2**, and **3**, respectively.

The secondary amine of *N*-methyl-1,2-ethanediamine be-

Table 4. Positional Parameters and B (eq) for [Pt(bpy)(Aten)]$(NO_3)_2 \cdot 2H_2O$ (**3**)

Atom	x	y	z	B (eq)/Å^2
Pt(1)	0.0102	0.26277(3)	0.0019	2.813(6)
O(1)	0.452(1)	0.415(2)	0.247(1)	7.5(4)
O(2)	0.278(1)	0.305(2)	0.183(1)	6.5(3)
O(3)	0.291(2)	0.541(2)	0.183(1)	8.3(4)
O(4)	0.851(1)	−0.051(2)	0.4608(9)	5.8(3)
O(5)	0.700(1)	0.090(2)	0.401(1)	7.1(3)
O(6)	0.868(2)	0.192(2)	0.471(2)	10.9(5)
O(7)	0.430(1)	0.058(2)	0.140(1)	7.3(4)
O(8)	0.955(2)	0.203(2)	0.738(1)	8.9(5)
N(1)	−0.067(1)	0.273(1)	0.111(1)	2.6(2)
N(2)	−0.104(1)	0.087(1)	−0.0237(7)	3.6(2)
N(3)	0.122(1)	0.237(1)	−0.102(1)	2.8(2)
N(4)	0.1230(9)	0.461(1)	0.0181(6)	3.0(2)
N(5)	0.344(1)	0.419(2)	0.2067(7)	5.2(3)
N(6)	0.807(1)	0.081(2)	0.4415(9)	5.0(3)
C(1)	−0.181(1)	0.197(1)	0.1005(9)	3.6(2)
C(2)	−0.266(2)	0.206(3)	0.164(1)	5.3(4)
C(3)	−0.229(2)	0.290(2)	0.243(1)	4.5(3)
C(4)	−0.109(1)	0.365(2)	0.250(1)	5.6(3)
C(5)	−0.039(1)	0.354(1)	0.1801(8)	4.1(2)
C(6)	−0.203(1)	0.088(1)	0.0240(8)	3.5(2)
C(7)	−0.310(2)	−0.005(2)	0.000(1)	5.9(4)
C(8)	−0.313(1)	−0.101(1)	−0.066(1)	4.8(3)
C(9)	−0.210(2)	−0.105(2)	−0.114(1)	5.3(3)
C(10)	−0.106(1)	−0.012(1)	−0.092(1)	4.3(3)
C(11)	0.191(1)	0.373(2)	−0.117(1)	4.1(3)
C(12)	0.2359(9)	0.443(1)	−0.0290(8)	3.1(2)
C(13)	0.033(1)	0.583(2)	−0.0191(7)	5.1(3)
C(14)	−0.070(1)	0.620(1)	0.0248(7)	3.3(2)
C(15)	−0.191(1)	0.557(1)	−0.0001(8)	3.6(2)
C(16)	−0.292(1)	0.574(1)	0.052(1)	3.9(2)
C(17)	−0.273(2)	0.670(1)	0.125(1)	4.8(3)
C(18)	−0.159(2)	0.746(1)	0.150(1)	3.7(3)
C(19)	−0.051(2)	0.724(1)	0.102(1)	3.5(2)
C(20)	−0.217(1)	0.470(1)	−0.0795(8)	3.4(2)
C(21)	−0.330(1)	0.393(1)	−0.100(1)	4.5(3)
C(22)	−0.430(1)	0.406(2)	−0.044(1)	5.5(4)
C(23)	−0.413(1)	0.496(2)	0.028(1)	4.0(3)
C(24)	0.063(1)	0.805(2)	0.130(1)	4.7(3)
C(25)	0.071(2)	0.903(2)	0.203(1)	7.3(4)
C(26)	−0.031(2)	0.922(2)	0.249(1)	5.8(4)
C(27)	−0.144(1)	0.846(1)	0.2229(9)	4.5(3)

Table 5. Comparison of Bond Lengths (Å) and Bond Angles (°) among [Pt(bpy)L_2]$(NO_3)_2 \cdot nH_2O$

L_2	Been	Npen	Aten
	Bonds		
Pt–N(1)	2.019(5)	2.030(7)	1.97(2)
Pt–N(2)	2.008(4)	2.032(9)	1.96(1)
Pt–N(3)	2.032(5)	2.046(9)	2.11(2)
Pt–N(4)	2.048(4)	2.056(9)	2.12(1)
	Angles		
N(1)–Pt–N(2)	81.1(2)	79.6(3)	83.7(4)
N(1)–Pt–N(3)	177.1(2)	177.1(3)	170.2(5)
N(1)–Pt–N(4)	98.6(2)	100.1(3)	99.1(4)
N(2)–Pt–N(3)	96.8(2)	97.5(4)	98.6(4)
N(2)–Pt–N(4)	179.3(2)	174.2(4)	174.4(4)
N(3)–Pt–N(4)	83.5(2)	82.8(3)	79.4(4)
Pt–N(1)–C(1)	113.6(4)	113.9(6)	110.4(9)
Pt–N(1)–C(5)	126.5(5)	125.7(5)	131.2(9)
Pt–N(2)–C(6)	114.2(4)	113.9(7)	110.4(9)
Pt–N(2)–C(10)	126.7(5)	124.9(8)	127.3(9)
Pt–N(3)–C(11)	110.2(4)	111.6(6)	112.3(9)
Pt–N(4)–C(12)	106.5(4)	105.8(7)	109.1(6)
Pt–N(4)–C(13)	114.7(3)	114.4(6)	104.2(8)

comes asymmetric upon coordination to a metal ion.[18] The five-membered chelate ring formed upon the coordination of ethanediamine is also asymmetric due to puckering. Therefore, there is diastereoisomerism due to the combination of the two asymmetic elements. Although the combination of (R, δ) and (S, λ) gives a pseudoequatorial orientation of the N-methyl group, the (R, λ) and (S, δ) combination gives the N-methyl group of a pseudo-axial orientation with respect to the five-membered chelate ring. For octahedral six-coordinated metal complexes, the conformers with (R, δ) or (S, λ) combination are generally preferred because of a smaller steric hindrance with the ligands at the apical positions. For square-planar metal complexes, the difference in energy between conformers with the set of (R, δ) or (S, λ) and those with (R, λ) and (S, δ) is small.[19] The presence of the bpy as the element of ternary complexes, however, exerts the N-alkyl-ethanediamine to take a conformation with the set of (R, λ) and (S, δ) combination. This had already been reported for [Pt(phen)(N-methylpropanediamine)]$^{2+}$ and [Pt(bpy)(N-methylethanediamine)]$^{2+}$.[20–22] The N-arylmethyl groups of **1**, **2**, and **3** have pseudo-axial orientations because if these groups take a pseudo-equatorial orientation, a strong intramolecular steric hindrance between the alkyl group and the hydrogen bonded to C(5) of bpy would occur. Therefore, these molecular cations can be regarded as a top, where the aromatic substituents rotate around the axis of N(4)–C(13) over the plane formed by the platinum-bpy moiety.

The torsion angles of Pt–N(4)–C(13)–C(14) are 170.6(4), 73.3(8), and 67(1)° for **1**, **2**, and **3**, respectively. Three rotamers can be distinguished when the alkyl group is higher than methyl(R–CH_2–).[18] The R group situates in a region far from the metal center in the *anti* rotamer and near to the other intramolecular ligand in (−)-*syn* rotamer, and covers itself in the (+)-*syn* rotamer for these conformers. These complexes, therefore, take *anti* for **1** but (−)-*syn* rotamer for **2** and **3**. This was driven by the large size of the aryl group for R. The projections of the complexes along the N(4)–C(13) bonds and perpendicular to this bond are shown in Fig. 3. In **1**, there is no stacking between the phenyl ring and the bipyridine ring, but in **2** and **3** significant stacking occurs between the aryl rings and the bipyridine rings. The area of stacking is larger for **3** than for **2**. For **2**, the naphthalene ring can take two conformations through a rotation around the C(13)–C(14) bond for the stacked form, but, significantly, the conformer which provides a larger stacking area between two possible conformers is observed.

We designate the six-membered rings of **1** to **3** as follows: A, one of the bipyridine rings of which pyridine moiety is *cis*

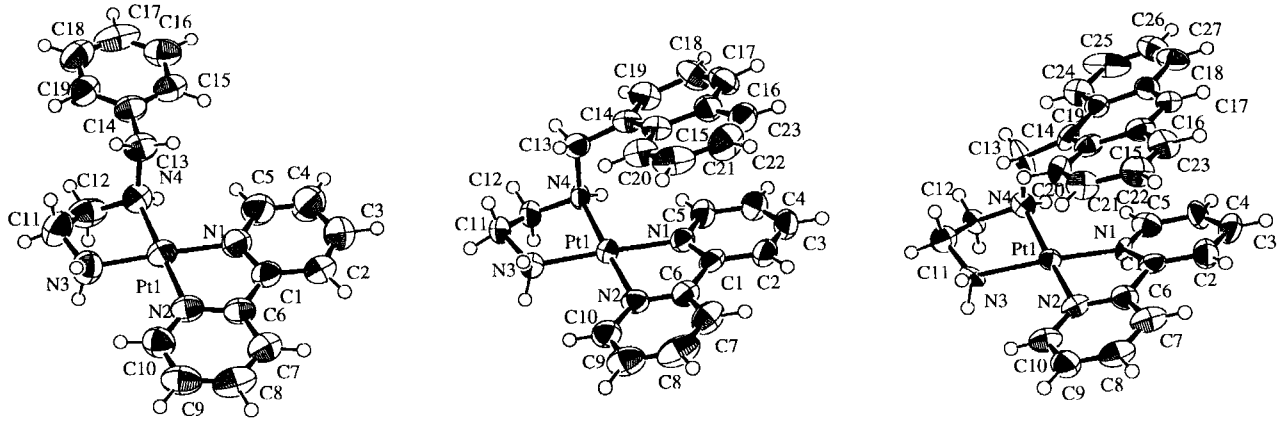

Fig. 2. Perspective drawings and labeling of non-hydrogen atoms of $[Pt(bpy)(Been)]^{2+}$ (**1**), $[Pt(bpy)(Npen)]^{2+}$ (**2**), and $[Pt(bpy)(Aten)]^{2+}$ (**3**).

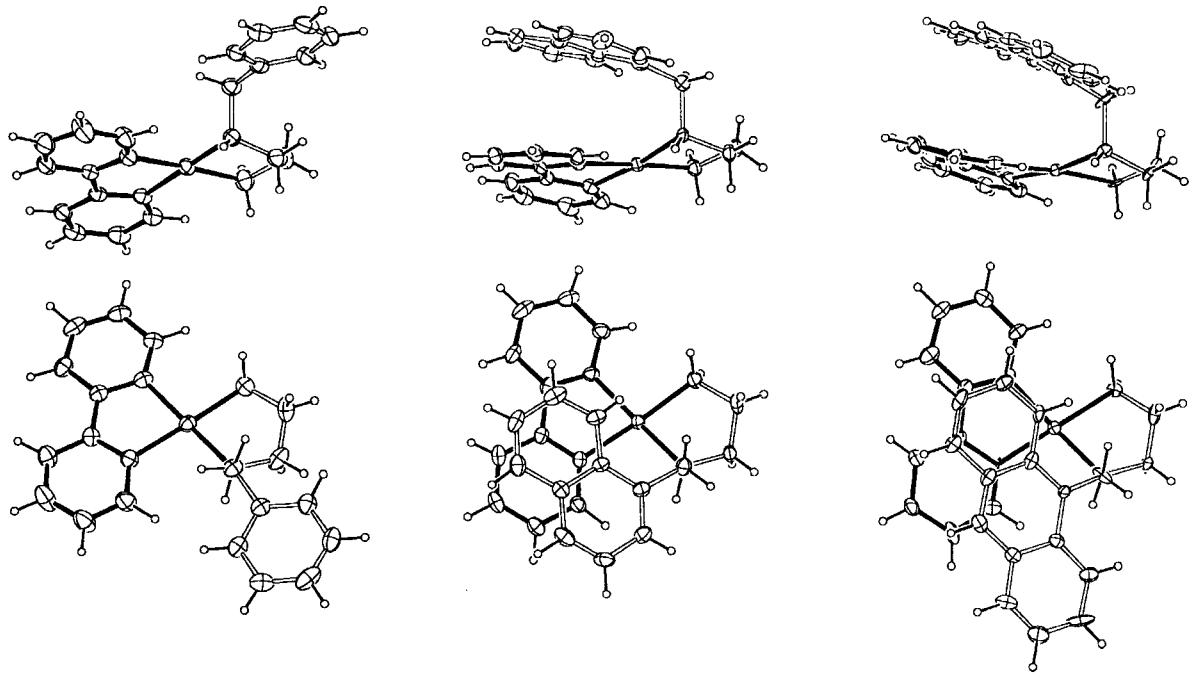

Fig. 3. The structures of $[Pt(bpy)(Been)]^{2+}$, $[Pt(bpy)(Npen)]^{2+}$, and $[Pt(bpy)(Aten)]^{2+}$ projected along and perpendicular to the axis of N(4)–C(13).

to the secondary amine; B, the other ring of bipyridine; C, the aromatic ring which is bonded to the methylene bridge, C(13), of the ethanediamine; D, the aromatic ring which is intramolecularly close to the bipyridine ring; E, the other aromatic ring which exists only in **3**.

In **2** and **3**, the closest separations of the centers of the rings are 3.49 and 3.7 Å between rings A and D and 3.86 and 3.59 Å between A and C, respectively. The dihedral angles between A and D are 12.05° and 7.45°, while those between A and C are 14.9° and 7.45° for **2** and **3** respectively. The interatomic distances less than 3.5 Å are 3.23, 3.29, 3.47, 3.28, 3.29, and 3.39 Å for N(1)···C(15), N(1)···C(20), C(4)···C(16), C(5)···C(14), C(5)···C(15), and C(5)···C(16), respectively in **2** and are 3.34, 3.20, 3.32, 3.47, 3.48, 3.45 Å for N(1)···C(14), N(1)···C(15), C(5)···C(14), C(5)···C(15), C(5)···C(19), and C(6)···C(21), respectively, in **3**. The difference arises from the torsion angles of the Pt–N(1)–C(13)–C(14), which is derived from the increased area of the interaction between the aromatic rings in **3**.

An intramolecular aromatic–aromatic interaction between an aromatic diimine, such as bpy and 1,10-phenanthroline, and the aromatic ring of α-amino acid has been evidenced by Cu(II) and Pd(II) complexes.[9,22–28] This is because these two aromatic rings are almost parallel and the separation of two rings are between 3.3 and 3.6 Å. However, the areas of the overlapping region of the two rings are different from the present complexes in which the arylmethyl groups are attached to nitrogens.

These aromatic rings also participate intermolecular stacking. The intermolecular stacking in **1** forms a four-layer stacking of phenyl–bpy–bpy–phenyl rings from four molecular ions, and bpy–bpy stacking is found between the molecular ions related by the inversion center to each other and the bpy–phenyl stacking is found between the molecular ions

related by translation along the *a*-axis; this array of stacking extends to the *a*-direction. The least-squares planes defined by nonhydrogen atoms take the closest contact between A and B (4.20 Å), B and B (4.20 Å), B and C (3.94 Å), as evaluated by the center of each ring and the interatomic distances less than 3.5 Å; they are 3.497(8) are 3.495(9) Å between C(1)···C(9) and C(6)···C(18), respectively, as shown in Fig. 4. The dihedral angle of the stacking bpy–bpy planes is less than 3°, but the dihedral angle between the central bpy and the bottom phenyl ring is 7.9—8.6°. One of the nitrates (N(4)O(4)O(5)O(6)) binds two complex ions related by the glide-plane directing *b*-axis, and the other fills the space with only one hydrogen bond to a complex cation.

The intermolecular stacking arrangements of **2** and **3** are shown in Figs. 5 and 6. The two asymmetric units of the complex cations form a face-to-face intermolecular stacking between molecular ions, which are related by the glide plane of (0,4,0) stepping to the *b*-axis in **2**. The distances between the center of each ring are 3.83 and 3.81 Å for the rings B and C and rings B and D while those between A and C, and A and D are 4.49 and 5.06 Å. The closest separation of nonhydrogen atoms is 3.27 Å for C(9)···C(23). The dihedral angles between B and C and B and D are 10.1° and 9.0°, respectively. The directions of the bpy and the naphthalene rings are almost perpendicular to each other. Thus, one of the bpy rings, B, is mainly involved in the intermolecular stacking.

In **3**, face-to-face intermolecular stacking occurs between the complex cations and that translated along the *c*-axis by 1 unit. Here, the distance between B and C, B and D, and B and E are 3.54, 3.86, 4.65 Å with a dihedral angle of 8.9, 8.3, and 7.6°, respectively, while the distances from the center of ring A to the center rings of C, D, and E are 5.78, 4.18, and 7.78 Å with dihedral angles of 12.1, 12.9, and 7.45°, respectively. The interatomic distances found for C(1)···C(26), C(1)···C(27), C(7)···C(17), C(7)···C(18), C(8)···C(15), C(8)···C(16), C(8)···C(17), C(9)···C(14), and C(9)···C(15) are 3.54(2), 3.50(2), 3.44(2), 3.39(2), 3.38(2), 3.39(2), 3.53(2), 3.41(2), and 3.44(2) Å, respectively. The directions of the long axes of anthracene and the bpy rings are almost parallel. Thus, in **3**, intermolecular stacking occurs mainly by the pyridine ring of bpy, B, which does not take part in the intramolecular stacking. In **2** and **3**, one of the pyridine rings (A) participates in intramolecular stacking and the other (B) takes a part in intermolecular stacking. It is noteworthy that the stacking in **2** and **3** occurs between the pyridyl group and the aromatic rings substituted to ethanediamine irrespective of whether they are intra- or intermolecular ones.

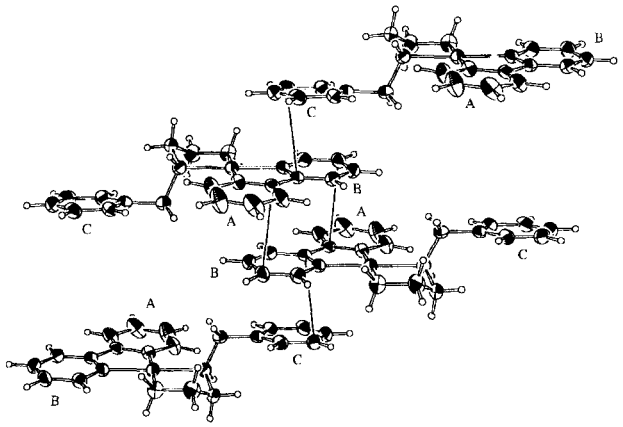

Fig. 4. Intermolecular stacking of $[Pt(bpy)(Been)]^{2+}$.

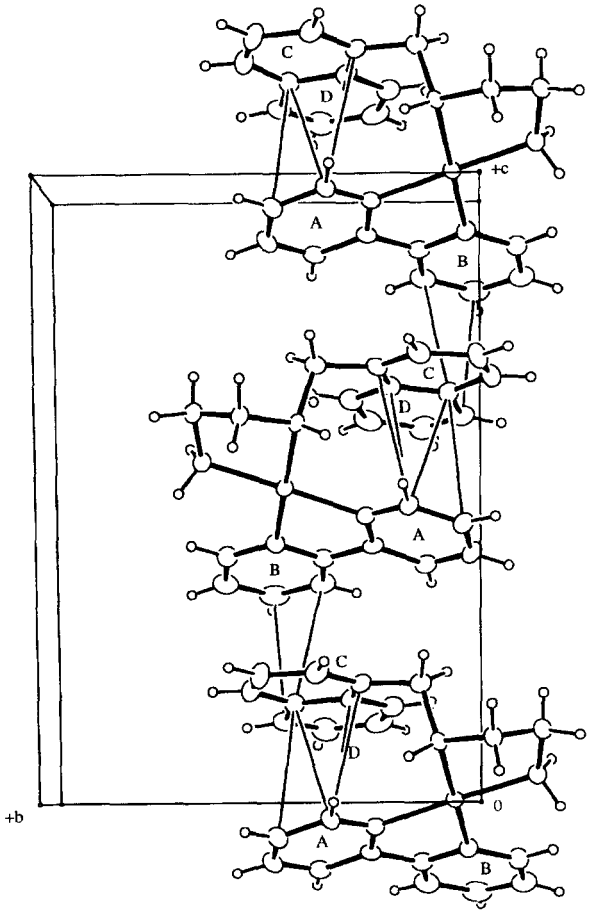

Fig. 5. Intermolecular stacking of $[Pt(bpy)(Npen)]^{2+}$.

The nitrate ions and two molecular water take part in hydrogen bond networks closely related for **2** and **3**. Schematic representations are shown in Fig. 7. The main hydrogen bond path is formed by two water oxygens (O(7) and O(8)) and one oxygen (O(1)) of one of the nitrates. Between the oxygen atoms of two nitrates and the oxygen atoms in the main path, an hydrogen bond is seen between O(3) and O(8), and O(7) attracts four additional oxygen atoms of nitrates (O(1), O(2), O(4) and O(6)). The hydrogen bonds from platinum complex cations are not seen with the oxygen atoms of the main path, but are seen with the oxygen atoms of the two nitrates. The difference between **2** and **3** is the arrangement of the complex ions around the main path: Two nitrates locate in a pseudo 2-fold spiral and the two nitrates bind different platinum complexes through N–H for **2**, but the oxygen atoms of the successive nitrates bind to the same platinum complex for **3**.

The aromatic regions of the ^{1}H NMR spectra of D_2O solutions of **1**, **2**, and **3** are shown in Fig. 8, where the signal

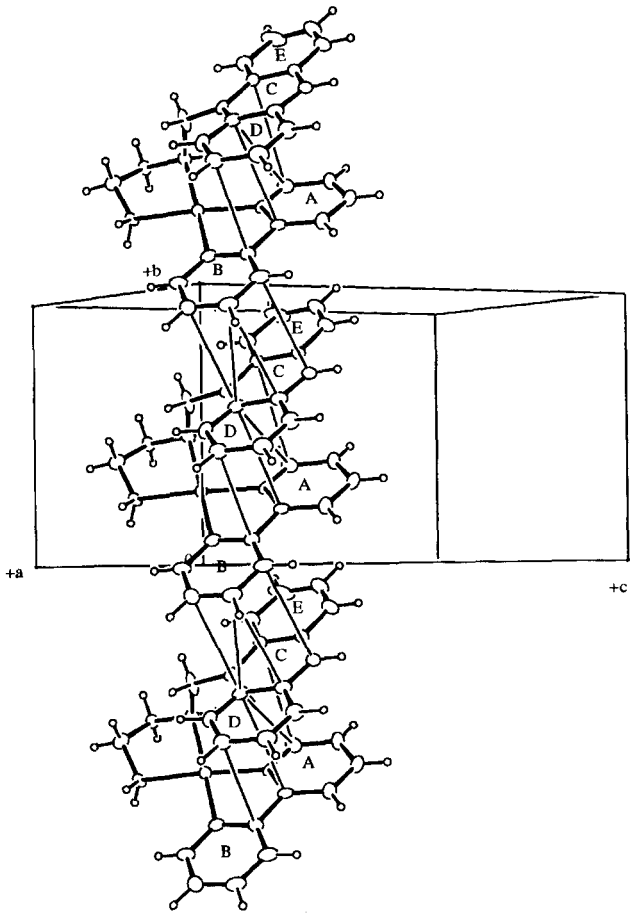

Fig. 6. Intermolecular stacking of $[Pt(bpy)(Aten)]^{2+}$.

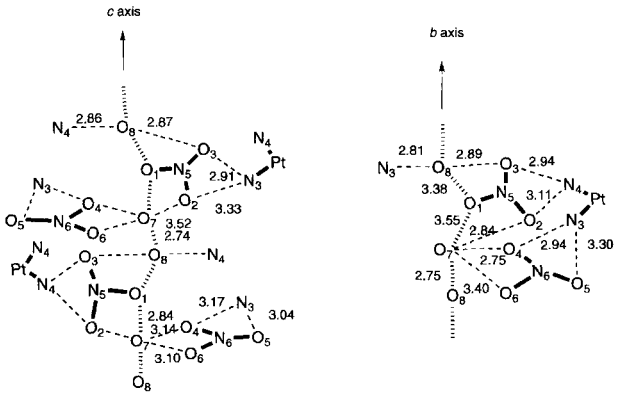

Fig. 7. Schematic comparison of hydrogen networks of $[Pt(bpy)(Npen)](NO_3)_2 \cdot 2H_2O$ (**2**) and $[Pt(bpy)(Aten)](NO_3)_2 \cdot 2H_2O$ (**3**).

marked with an asterisk is assigned to each aryl ring proton based on the ^1H-^1H COSY spectra. The signals for the protons attached to one ring (H_3–H_6) of the bipyridine moiety appeared at a higher field than those of the corresponding $[Pt(bpy)(en)]^{2+}$. The protons on the other ring of bipyridine are denoted as $H_{3'}$–$H_{6'}$. Though **1** showed only a small concentration dependency, **2** and **3** showed a significant concentration dependency. ^1H NMR spectra were recorded at various concentrations, and each chemical shift intrinsic to the isolated complex ion was estimated from plots of the chemical shift vs. the employed concentration by extrapolating the concentration to 0. These chemical shifts are tabulated in Table 6.

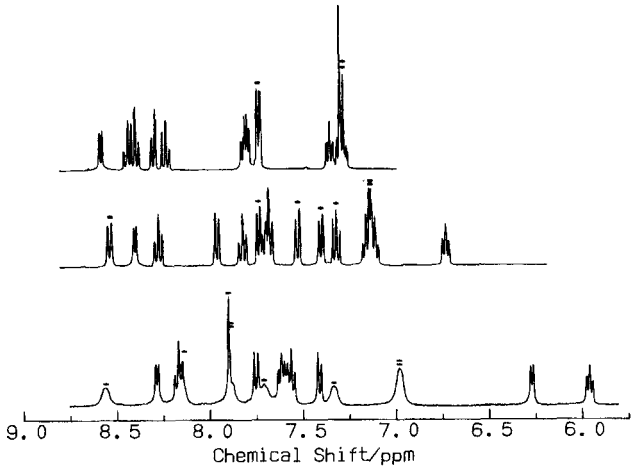

Fig. 8. Aromatic region of ^1H NMR spectra of D_2O solutions of $[Pt(bpy)(Been)]^{2+}$ (**1**), top; $[Pt(bpy)(Npen)]^{2+}$ (**2**), middle; and $[Pt(bpy)(Aten)]^{2+}$ (**3**), bottom. An asterisk indicates a signal due to each proton of the aryl groups. The chemical shifts and assignments are as follows, where bpy, phe, nap, and ant corresponds to bipyridine, phenyl, naphthyl, and anthryl, respectively: **1** (concn = 53 mM); 7.30 (mult, phe H_3, H_4, and H_5), 7.36 (t, bpy H_5), 7.74 (d, phe H_2 and H_6), 7.80 (d, bpy H_6), 7.82 (t, bpy $H_{5'}$), 8.24 (t, bpy H_4), 8.31 (d, bpy H_3), 8.40 (d, bpy $H_{3'}$), 8.45 (t, bpy $H_{4'}$), 8.59 (d, bpy $H_{6'}$): **2** (concn = 35 mM); 6.74 (t, bpy H_5), 7.12 (t, nap H_7), 7.15 (d, bpy H_6), 7.17 (t, nap H_6), 7.32 (t, nap H_3), 7.42 (d, nap H_5), 7.54 (d, nap H_4), 7.68 (d, bpy H_3), 7.71 (t, bpy $H_{5'}$), 7.75 (d, nap H_2), 7.83 (t, bpy H_4), 7.97 (d, bpy $H_{3'}$), 8.28 (t, bpy $H_{4'}$), 8.41 (d, bpy $H_{6'}$), 8.55 (d, nap H_8): **3** (concn = 15 mM); 5.97 (t, bpy H_5), 6.29 (d, bpy H_6), 6.96 (br, ant H_6 and H_7), 7.35 (br, ant H_5), 7.43 (d, bpy H_3), 7.57 (t, bpy H_4), 7.63 (t, bpy $H_{5'}$), 7.72 (br, ant H_3), 7.77 (d, bpy $H_{3'}$), 7.89 (br, ant H_2), 7.91 (s, ant H_{10}), ca. 7.91 (br, ant H_4), 8.16 (br, ant H_1), 8.18 (d, bpy $H_{4'}$), 8.30 (d, bpy $H_{6'}$), 8.58 (br, ant H_8).

The chemical shift of H_6 of bpy moved upfield by $\delta = 0.87$,

Table 6. ^1H NMR Chemical Shifts of bpy in $[Pt(bpy)(L_2)]^{2+}$ Deduced from the Extrapolation to Infinite Dilution[a)]

L_2	H_3	H_4	H_5	H_6	$H_{3'}$	$H_{4'}$	$H_{5'}$	$H_{6'}$
en	8.44	8.45	7.82	8.66				
Been	8.30	8.24	7.36	7.79	8.39	8.43	7.81	8.58
Npen	7.90	7.95	6.86	7.31	8.16	8.36	7.74	8.51
Aten	7.80	7.80	6.23	6.61	8.10	8.34	7.73	8.51

a) The chemical shifts for the aryl groups at infinite dilution are as follows: $[Pt(bpy)(Been)]^{2+}$: H_2 and H_6, 7.73; H_3, H_4, and H_5, 7.29. $[Pt(bpy)(Npen)]^{2+}$: H_8, 8.75; H_2, 7.91; H_4, 7.75; H_5, 7.63; H_3, 7.47; H_6, 7.33; H_7, 7.29. $[Pt(bpy)(Aten)]^{2+}$: H_8, 8.97; H_1, 8.49; H_{10}, 8.43; H_4, 8.21, H_2, 7.88; H_3, 7.76; H_5, 7.72; H_6 and H_7; 7.22 ppm.

1.35, and 2.05 compared to that of the en complex for **1**, **2**, and **3**, respectively. A similar trend is seen for H_5 with less magnitude. H_3 and H_4 of **1** show small shifts from those of the en complexes, but those of **2** and **3** show significant shifts. These upfield shifts are caused by a ring-current effect of the aromatic rings of the *syn*(−)-rotamer for **1**, **2**, and **3** because the hydrogens of the half pyridine ring of bipyridine are under the effect;[29] these arrangements are in agreement with those in the crystals for **2** and **3**.

Thus, the structures of **2** and **3**, deduced from the ^{1}H NMR spectra, are in agreement with those found in the crystal states. However, the structure of **1** in the crystal has different conformations from that in solution. This discrepancy is a consequence of the difference in the magnitude of the overlapping between the aromatic rings. For **2** and **3**, the size is large enough to maintain the stacked structures both in solution and in the crystal states, but the small size of the phenyl ring in **1** does not afford the intramolecular stacking strongly enough to be kept in the crystal, where crystal packing makes intermolecular π–π stackings.

The present study has shown that the aromatic–aromatic ring stacking occurs efficiently between an aromatic ring of *N*-arylmethyl-1,2-ethanediamine and the intramolecular bipyridine ring in square planar complexes. The stacking is effected mainly by a van der Waals interaction[30] and is substantiated by charge transfer from the aryl group to the coordinated bipyridine.[9] In aqueous solution, the formation of the intramolecular stacking of apoplar aromatic rings releases water molecules from the aromatic surfaces to the bulk, and is favored both enthalpically and entropically in enegy.[30]

This work was partly supported by a Grant-in-Aid for Scientific Research No. 04640583 from the Ministry of Education, Science, and Culture.

References

1 E. Dubler, U. K. Häring, K. H. Scheller, P. Baltzer, and H. Sigel, *Inorg. Chem.*, **23**, 3785 (1984).

2 H. Sigel, R. Malini-Balakrishnan, and U. K. Häring, *J. Am. Chem. Soc.*, **107**, 5137 (1985).

3 R. Malini-Balakrishnan, K. H. Scheller, U. K. Häring, and R. Tribolet, *Inorg. Chem.*, **24**, 2067 (1985).

4 O. Yamauchi, K. Tsujide, and A. Odani, *J. Am. Chem. Soc.*, **107**, 659 (1985).

5 O. Yamauchi and A. Odani, *J. Am. Chem. Soc.*, **107**, 5938 (1985).

6 A. Odani, S. Deguchi, and O. Yamauchi, *Inorg. Chem.*, **25**, 62 (1986).

7 A. Odani and O. Yamauchi, *Nihon-Kagaku Kaishi*, **1987**, 336.

8 O. Yamauchi and A. Odani, *Nihon-Kagaku Kaishi*, **1988**, 369.

9 T. Sugimori, H. Masuda, N. Ohata, K. Koiwai, A. Odani, and O. Yamauchi, *Inorg. Chem.*, **36**, 576 (1997), and references therein.

10 S. J. Lippard, *Acc. Chem. Res.*, **11**, 211 (1978).

11 O. Yamauchi, A. Odani, R. Shimata, and Y. Kosaka, *Inorg. Chem.*, **25**, 3337 (1986).

12 A. Odani, R. Shimata, H. Masuda, and O. Yamauchi, *Inorg. Chem.*, **30**, 2133 (1991).

13 G. T. Morgan and F. H. Burstall, *J. Chem. Soc.*, **1934**, 965.

14 T. W. Hambley, C. J. Hawkins, J. Martin, J. A. Palmer, and M. R. Snow, *Aust. J. Chem.*, **34**, 2505 (1981).

15 "Crystal Structure Analysis Package," Molecular Structure Corporation (1985 & 1992).

16 R. H. Herber, M. Croft, M. J. Coyer, B. Bilash, and A. Sahiner, *Inorg. Chem.*, **33**, 3422 (1994).

17 H. Masuda and O. Yamauchi, *Inorg. Chim. Acta*, **136**, L29 (1987).

18 H. Kurosaki, S. Koga, and M. Goto, *Bull. Chem. Soc. Jpn.*, **68**, 843 (1995).

19 C. J. Hawkins and J. A. Palmer, *Coord. Chem. Rev.*, **44**, 1 (1982).

20 Bosnich and E. A. Sullivan, *Inorg. Chem.*, **14**, 2768 (1975).

21 Y. Nakayama, K. Matsumoto, S. Ooi, and H. Kuroya, *Bull. Chem. Soc. Jpn.*, **50**, 2304 (1977).

22 K. Aoki and H. Yamazaki, *J. Chem. Soc., Dalton Trans.*, **1987**, 2017.

23 M. Masuda, O. Matsumoto, A. Odani, and O. Yamauchi, *Nihon-Kagaku Kaishi*, **1988**, 783.

24 O. Yamauchi, A. Odani, T. Kohzuma, H. Masuda, K. Toriumi, and K. Saito, *Inorg. Chem.*, **28**, 4066 (1989).

25 T. Sugimori, K. Shibakawa, H. Masuda, A. Odani, and O. Yamauchi, *Inorg. Chem.*, **32**, 4951 (1993).

26 T. Sugimori, H. Masuda, and O. Yamauchi, *Bull. Chem. Soc. Jpn.*, **67**, 131 (1994).

27 F. Zhang, A. Odani, H. Masuda, and O. Yamauchi, *Inorg. Chem.*, **35**, 7184 (1996).

28 F. Zhang, T. Yajima, H. Masuda, A. Odani, and O. Yamauchi, *Inorg. Chem.*, **36**, 5777 (1997).

29 a) C. E. Johnson, Jr., and F. A. Bovey, *J. Chem. Phys.*, **29**, 1012 (1985). b) R. J. Abraham, S. C. M. Fell, and K. M. Smith, *Org. Magn. Reson.*, **9**, 367 (1977).

30 D. B. Smithrud and F. Diederich, *J. Am. Chem. Soc.*, **112**, 339 (1990).